Jurnal Teknik Informatika (JUTIF) Vol. 6, No. 2, April 2025, Page. 981-994
P-ISSN: 2723-3863 https://jutif.if.unsoed.ac.id
E-ISSN: 2723-3871 DOI: https://doi.org/10.52436/1.jutif.2025.6.2.4315

Tuberculosis Diagnosis From X-Ray Images Using Deep Learning And Contrast Enhancement Techniques

Vita Melati Risma*[1], Ema Utami[2]

[1,2]Magister of Informatics, Amikom University, Yogyakarta, Indonesia

Email: [1]vitamelatirisma@students.amikom.ac.id

Received : Jan 13, 2025; Revised : May 3, 2025; Accepted : May 7, 2025; Published : May 17, 2025

Abstract

Tuberculosis (TB) is an infectious disease that poses a global health threat. Early diagnosis through chest X-ray (CXR) imaging is effective in reducing transmission and improving patient recovery rates. However, the limited number of radiologists in high TB burden areas hampers rapid and accurate detection. This study aims to improve TB diagnosis accuracy using deep learning models. Convolutional Neural Networks (CNN) are applied to analyze CXR images to support automated detection in regions with limited radiology personnel. The method involves image processing using Contrast Limited Adaptive Histogram Equalization (CLAHE) to enhance image quality. A public dataset consisting of 2,188 images was used, with preprocessing steps including resizing, normalization, and augmentation. The DenseNet201 model was employed as the main architecture, trained for 10 epochs with various batch sizes to evaluate its performance. Results show that the combination of CLAHE and DenseNet201 achieved the highest accuracy of 94.84%. Image quality enhancement with CLAHE proved to improve accuracy compared to models without preprocessing. This research contributes to enhancing the efficiency of automated early TB detection, reducing reliance on radiologists, and accelerating clinical decision-making.

Keywords : *Chest X-ray, CLAHE, CNN, DenseNet201, Tuberculosis.*

1. INTRODUCTION

Tuberculosis (TB) is a highly contagious and potentially fatal disease. It is caused by the bacterium Mycobacterium tuberculosis, which primarily attacks the lungs and can spread through the air when an infected person coughs, sneezes, or spits [1]. Tuberculosis can cause serious respiratory problems, such as chronic coughing and shortness of breath [2]. Tuberculosis remains a significant global health challenge. In 2019, approximately 9.96 million TB cases were recorded worldwide, with the Southeast Asia region accounting for 44% of new cases, according to the World Health Organization (WHO) [3]. In Indonesia, TB is one of the major public health issues, with an estimated 351,936 new cases in 2020, mostly concentrated in the provinces of West Java, East Java, and Central Java [4]. Chest X-ray (CXR)-based TB diagnosis is a commonly used method; however, its interpretation still heavily relies on radiological expertise, which is limited in number, especially in high-prevalence areas.

Deep learning utilizes artificial neural network concepts to recognize and learn patterns in data[5]. One of the most well-known deep learning architectures for image classification is the Convolutional Neural Network (CNN), which is highly effective in analyzing two-dimensional data such as images [6]. CNNs have been successfully applied in various fields with accuracy rates exceeding 90%, including medical image analysis [7], plant disease identification [8], handwriting recognition [9] and facial recognition [10]

Previous studies have shown that CNNs are effective in tuberculosis (TB) analysis. For example, one study [11] employed ConvNet, Xception, ResNet50, and VGG16 models to detect TB, achieving

P-ISSN: 2723-3863 https://jutif.if.unsoed.ac.id
E-ISSN: 2723-3871 DOI: https://doi.org/10.52436/1.jutif.2025.6.2.4315

90% accuracy. Another study [12] applied transfer learning with CNNs and found that the DenseNet201 model outperformed other CNN architectures on segmented datasets, with classification accuracy and precision of 98.6% and 98.57%, respectively. Research [13] further demonstrated that CNNs are effective in identifying complex patterns in medical images, including chest X-rays (CXR) for TB detection. A follow-up study [14] explored multiple EfficientNet models for TB diagnosis, with EfficientNet-B4 achieving the best results among its variants 92.33% accuracy on the Montgomery dataset and 94.35% on the Shenzhen dataset.

However, these studies used relatively small datasets, which makes the models prone to overfitting. Although CNNs already demonstrate high accuracy, their performance can be further improved with preprocessing steps such as contrast enhancement [15]. The purpose of contrast enhancement is to adjust pixel brightness levels to improve visual quality, which is critical in digital image processing, pattern detection, and computer vision tasks [16]. Low-contrast images, often caused by poor equipment or inadequate lighting, can hinder analysis and object recognition. Thus, contrast enhancement becomes an essential step prior to further processing.

In medical images such as X-rays, image quality is often affected by various factors including suboptimal equipment, operator errors, and patient conditions, which may result in blurred images with insufficient detail and poor contrast [17]. These issues can significantly impact the accuracy of CNN-based analysis. Therefore, enhancing image quality prior to applying CNN is crucial. One effective technique is Contrast Limited Adaptive Histogram Equalization (CLAHE), which improves image contrast without causing over-enhancement [18] . CLAHE works by dividing the image into small regions (tiles) and enhancing the contrast of each part independently, resulting in improved overall image quality [19] [20]. Several previous studies have demonstrated the effectiveness of CLAHE in improving image quality, such as those in [21], [22], and [23]. For instance, [24] proposed a CNN model for pneumonia detection that achieved 94% accuracy, while [11] suggested the use of ResNet50 and VGG16 architectures.

This study aims to implement CLAHE and CNN for tuberculosis classification in chest X-ray images [25]. By employing a more advanced CNN architecture, DenseNet201, the study seeks to improve diagnostic accuracy for TB. It is expected that this approach can facilitate the X-ray image analysis process for physicians and radiologists, minimizing interpretation errors and increasing the chances of patient recovery.

2. RESEARCH METHODS

The research method provides an overview of the stages of the study conducted from beginning to end. The research flow can be seen in the following Figure 1.

The DenseNet201 model was chosen for this study due to its unique architecture designed to enhance the efficiency of information and feature flow through dense connectivity between layers. By directly connecting each layer to all previous layers, DenseNet201 not only reduces feature redundancy but also ensures optimal use of important information, which is particularly useful in handling the visual complexity of X-ray images.

On the other hand, CLAHE (Contrast Limited Adaptive Histogram Equalization) was chosen because it can enhance contrast adaptively without causing noise overamplification, which often occurs with standard Histogram Equalization (HE) or Adaptive Histogram Equalization (AHE). By operating on small blocks of the image, CLAHE preserves local details, allowing for the detection of subtle features in the lungs that are crucial for tuberculosis diagnosis. This method is also more robust to lighting variations within X-ray datasets, resulting in more consistent images for feature extraction by DenseNet201. The combination of CLAHE and CNN ensures that contrast enhancement does not

P-ISSN: 2723-3863
E-ISSN: 2723-3871
Vol. 6, No. 2, April 2025, Page. 981-994
https://jutif.if.unsoed.ac.id
DOI: https://doi.org/10.52436/1.jutif.2025.6.2.4315

compromise important information, thereby supporting the model's accuracy in detecting abnormalities more effectively.

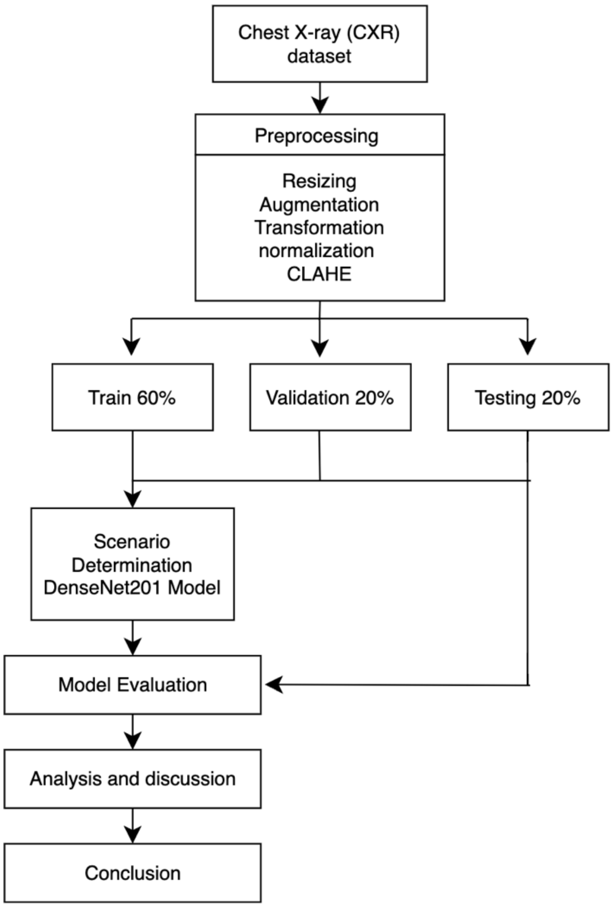

Figure 1. Research Flow

2.1. Dataset

Data collection in this study was carried out by searching for relevant data through the internet, particularly datasets that are key elements of the research. The dataset used consists of chest X-ray images obtained from two main sources. The first source is the online platform Kaggle, while the second source is a collection of X-ray images obtained from the study [11]. Overall, this dataset includes 2,188 X-ray images divided into two categories: normal and tuberculosis. Example X-ray images from both categories are shown in Figure 2 and Figure 3.

Figure 2. Normal X-Ray Image

Figure 3. X-Ray Image Of Tuberculosis

Vol. 6, No. 2, April 2025, Page. 981-994
https://jutif.if.unsoed.ac.id
DOI: https://doi.org/10.52436/1.jutif.2025.6.2.4315

2.2. Preprocessing

Data preprocessing is a crucial stage in this study to ensure the dataset quality is optimal before being used for training the classification model. The first step in preprocessing is resizing the images, as the original image sizes vary. All images are resized to 255×255 pixels to achieve consistent dimensions compatible with the architecture of the model. Next, data augmentation is applied to increase dataset variability, enabling the model to recognize a wider range of patterns and reducing the risk of overfitting. Augmentation techniques used include random horizontal and vertical flipping, random rotation, and conversion of images into tensors. These techniques enhance data diversity, allowing the model to learn object recognition across various orientations and conditions, which is essential for improving its generalization capability. Moreover, since deep learning models require inputs in the form of numerical tensors rather than standard images, converting the images to tensors ensures that the data is suitable for further processing by the model. The final step in preprocessing is image normalization, which is performed using the mean and standard deviation values calculated from a similar dataset. This normalization transforms pixel values to a more uniform distribution, helping to accelerate convergence and improve model accuracy.

The dataset is then divided into three main subsets: training data (60% of the total), validation data (20%), and testing data (20%). This split is performed using the train_test_split parameter on the variables x and y. The training data is used to build the model, validation data is used to monitor model performance during training, and testing data evaluates final model performance on unseen, real-world-like data.As an additional step, a visual exploration of the dataset is conducted by displaying sample images from each disease class to ensure data diversity, including after augmentation. The model is then trained for 10 epochs using varying batch sizes 16, 32, and 64. This number of epochs is chosen to balance training time and model convergence. A smaller batch size (16) leads to more frequent weight updates, while a larger batch size (64) speeds up training but increases the risk of overfitting. During training, training data is used for optimization, and validation data is used to monitor performance and prevent overfitting. Evaluation is conducted every few epochs, and after training, the model is assessed using the test data to measure its accuracy on previously unseen data. These steps are designed to ensure that the dataset used is of high quality, thus supporting optimal model training.

2.3. Contrast Limited Adaptive Histogram Equalization (CLAHE)

CLAHE (Contrast Limited Adaptive Histogram Equalization) is an advanced version of the adaptive histogram equalization method designed to enhance image contrast adaptively without losing essential details or introducing unwanted noise [26]. This technique operates by equalizing the histogram of small image blocks independently while applying limitations or clipping to the histogram. This prevents excessive contrast enhancement in homogeneous areas or regions with high noise levels. This approach effectively minimizes the risk of significant noise amplification, thereby preserving the overall quality of the image.

The steps of CLAHE [27] can be described as follows:

- Divide the input image into small, continuous, and non-overlapping blocks, typically 8×8 pixels in size or adjusted according to configuration.
- Calculate the histogram for each image block and apply a threshold to clip the histogram before computing the PDF (Probability Density Function) and CDF (Cumulative Distribution Function), limiting the gradient of the transformation function.
- Redistribute pixel values by allocating adjusted pixel values evenly across the histogram.
- Perform local histogram equalization on each block.
- Use linear interpolation to reconstruct pixel values based on the intensity level mapping of the surrounding sample points.

Vol. 6, No. 2, April 2025, Page. 981-994
https://jutif.if.unsoed.ac.id
DOI: https://doi.org/10.52436/1.jutif.2025.6.2.4315

2.4. Convolution Neural Networks (CNN)

Convolutional Neural Network (CNN) is a highly efficient deep learning algorithm for processing structured two-dimensional data, such as images [28]. With its hierarchical approach, CNN is capable of analyzing information from the initial convolution layers to the final layers, enabling classification with high accuracy, as seen in the context of Pekalongan batik pattern classification. Each convolutional layer uses the output of the previous layer as input, allowing the network to extract increasingly complex features as the depth of the network increases. Fully connected layers and activation functions like ReLU (Rectified Linear Unit) play an important role in processing these features to produce class predictions or image labels[29]. The workflow of CNN, as illustrated in Figure 3, provides a clear visual representation of how CNN works in this context, from the initial image processing to the final classification result.

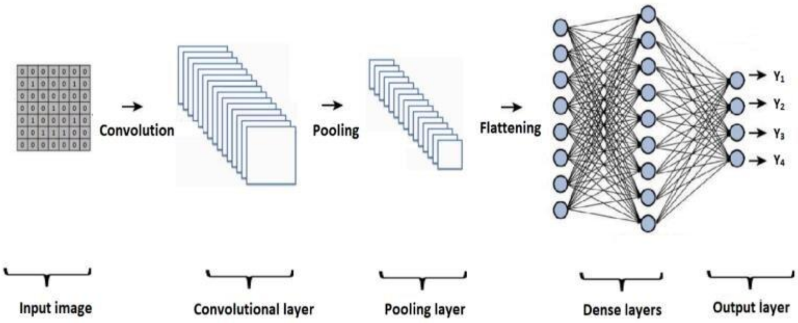

Figure 4. CNN Process

2.5. DenseNet201

After the data undergoes the necessary preprocessing steps, the next step is to train the CNN model, which involves feature extraction and classification. This study uses the Convolutional Neural Network (CNN) algorithm with the DenseNet201 architecture, which is well-known for image classification tasks.

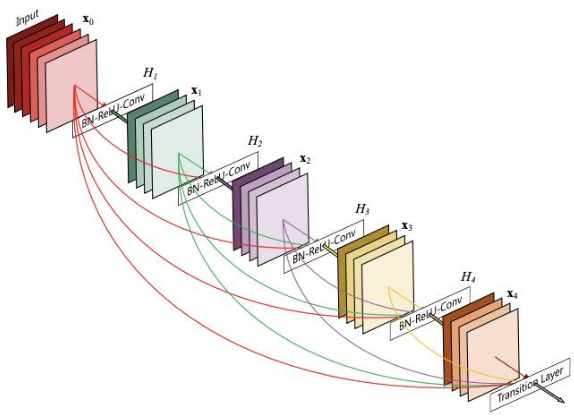

Figure 5. DenseNet architecture [30]

DenseNet201 (Dense Convolutional Network) is one of the variants of the DenseNet architecture designed to deepen deep learning networks by optimizing training efficiency and feature utilization. Like other DenseNet architectures, DenseNet201 uses a dense connectivity approach, where each layer is directly connected to all subsequent layers. This means that the output of each layer is used as input for all deeper layers, without excessive redundancy. This approach allows for smoother data and gradient

Vol. 6, No. 2, April 2025, Page. 981-994
https://jutif.if.unsoed.ac.id
DOI: https://doi.org/10.52436/1.jutif.2025.6.2.4315

flow throughout the network, addressing the vanishing gradient problem and improving the reuse of relevant features. With 201 layers, DenseNet201 provides stronger representational capabilities compared to versions with fewer layers, such as DenseNet121, making it highly suitable for handling datasets with high visual complexity, such as X-ray images in medical diagnosis. The image of the densenet architecture can be seen in figure 5.

2.6. Testing Scenario

In this study, two testing scenarios were implemented to evaluate the model's performance. The first scenario involves experimenting with the DenseNet201 model without using CLAHE, while the second scenario incorporates the use of CLAHE in the DenseNet201 model. Both scenarios were tested with various batch sizes to observe their impact on the model's accuracy and training stability. The early stopping technique was applied to prevent overfitting by halting training when the model's performance on the validation data begins to decline. This approach ensures efficient training while maintaining the effectiveness of the training process. These scenarios are designed to optimize training conditions, allowing for a deeper analysis of the model's ability to generalize across different settings.

2.7. Model Evaluation

Model evaluation is performed using a confusion matrix. The parameters analyzed include accuracy, precision, recall, and F1-score, which are calculated based on Equations (1), (2), (3), and (4). TP refers to True Positive, FP refers to False Positive, TN refers to True Negative, and FN refers to False Negative [31].

Accuracy measures how close the obtained results are to the true values. Precision indicates the relevance of the data retrieved with the information needed. Recall reflects the success in identifying and retrieving relevant information. Meanwhile, the F1-score is the harmonic mean of precision and recall, providing a balanced view of the model's performance [32].

$$\text{Accuracy} = \frac{TP+TN}{TP+TN+FP+FN} \quad (1)$$

$$\text{Precision} = \frac{TP}{TP+FP} \quad (2)$$

$$\text{Recall} = \frac{TP}{TP+FN} \quad (3)$$

$$\text{F1}-\text{Score} = \frac{2x\ Recall\ x\ Precision}{Recall+Precision} \quad (4)$$

3. RESULTS

This chapter discusses the experimental results conducted to evaluate the performance of the DenseNet201 model in two different scenarios. The first scenario uses the early stopping technique and batch size variations without applying the CLAHE image preprocessing method. The second scenario also employs the early stopping technique and batch size variations, but with the CLAHE image preprocessing method applied. The model's performance is evaluated by measuring several metrics, including accuracy, loss, validation accuracy, and validation loss, as well as other evaluation metrics such as precision, recall, and F1-score.

3.1. Dataset

After the preprocessing process, the dataset consisting of 2.188 X-ray images of size 255x255 pixels was prepared for the validation, training, and testing stages of the tuberculosis diagnosis model. In the first scenario, the model uses the original dataset without any modifications. Meanwhile, in the second scenario, the dataset is generated by applying a contrast enhancement method using Contrast Limited Adaptive Histogram Equalization (CLAHE) on the original dataset. This augmented dataset

Vol. 6, No. 2, April 2025, Page. 981-994
https://jutif.if.unsoed.ac.id
DOI: https://doi.org/10.52436/1.jutif.2025.6.2.4315

contains the same number of images as the original dataset. The use of this contrast-enhanced dataset aims to evaluate the impact of the contrast enhancement method on classification accuracy and to compare the classification results between the two scenarios.

3.2. Scenario 1

The first experiment was conducted by varying the batch size (16, 32, 64) and using the early stopping technique for the DenseNet201 model without using CLAHE. The results of this experiment can be seen in Table 1.

Table 1. Densenet201 Model Without CLAHE Implementation

Batch Size	Epoch Stop	Accuracy	Loss	Accuracy Validation	Loss Validation	Densenet201 Accuracy
16	10	93.58%	0.1901	88.72%	0.3218	91.25%
32	10	97.61%	0.0646	90.24%	0.4870	90.01%
64	10	98.70%	0.0326	86.29%	0.5340	92.42%

Based on the results of the experiment in Scenario 1, the DenseNet201 model with a batch size of 64 performed the best, achieving the highest validation accuracy of 92.42%. This result indicates that increasing the batch size does not consistently improve the performance of the DenseNet201 model.

3.3. Scenario 2

The second experiment was conducted by varying the batch size (16, 32, 64) and using the early stopping technique for the DenseNet201 model with CLAHE. The results of this experiment can be seen in Table 2.

Table 2. Densenet201 Model With CLAHE Implementation

Batch Size	Epoch Stop	Accuracy	Loss	Accuracy Validation	Loss Validation	Densenet201 Accuracy
16	10	96.30%	0.1027	89.33%	0.2608	94.84%
32	10	96.62%	0.0875	85.06%	0.5405	90.33%
64	10	99.08%	0.0288	65.24%	2.6764	88.18%

Based on the results of the experiment in Scenario 2, the DenseNet201 model with the application of CLAHE and a batch size of 16 performed the best, achieving the highest validation accuracy of 94.84%. This result indicates that increasing the batch size tends to reduce the performance of the DenseNet201 model.

3.4. Test Results

This experiment was conducted using two main scenarios: applying the DenseNet201 model with and without the use of CLAHE (Contrast Limited Adaptive Histogram Equalization) to analyze the effect of preprocessing on model performance. Additionally, the experiment involved variations in batch size to evaluate how this parameter impacts model accuracy under each scenario. The results indicate that applying CLAHE to DenseNet201 significantly improves classification performance, with the highest accuracy of 94.84% achieved at a batch size of 16. The CLAHE technique enhances image quality by improving contrast and sharpening details, which is particularly useful for detecting subtle

P-ISSN: 2723-3863 https://jutif.if.unsoed.ac.id
E-ISSN: 2723-3871 DOI: https://doi.org/10.52436/1.jutif.2025.6.2.4315

visual patterns. This allows the model to learn more effectively from image features, leading to a notable increase in accuracy.

In contrast, in the scenario without CLAHE, the model's accuracy tends to be lower, indicating that advanced preprocessing plays a critical role in enabling the model to capture more relevant features. This significant improvement in accuracy is further highlighted when comparing these results with a previous study conducted by [11], where the model achieved only 90% accuracy. That study did not provide detailed precision and recall values for each class, while in this study, the application of CLAHE not only improved accuracy but also enhanced the model's consistency when handling validation data. DenseNet201 with CLAHE demonstrated higher accuracy and more stable performance, despite variations in batch size. The batch size of 16, though smaller, yielded the best performance, indicating that more frequent weight updates helped the model learn more effectively.

The experimental results also show that the model did not suffer from significant overfitting or underfitting. In the scenario with CLAHE, although there was an increase in training accuracy, the validation accuracy showed similar improvements, suggesting that the model was able to generalize well without overfitting. This is also reflected in the comparison of loss and accuracy, where the training and validation curves followed a similar and convergent trend by the end of training. If overfitting had occurred, the validation loss would have remained high while the training accuracy continued to increase something not observed in this experiment. Conversely, signs of underfitting, where training loss remains high and accuracy stays low, were also absent. The model demonstrated good convergence, and the highest accuracy achieved with a batch size of 16 further supports the indication that the model learned effectively and was not hindered by training parameters.

3.5. Visualization of Results

To provide a deeper understanding of the performance of the tested model, several visualizations are presented to illustrate various aspects of the model evaluation. Figure 6 shows the accuracy graph during the training and validation processes, illustrating how the model learns from the data and gradually reaches convergence. This graph provides insights into the model's stability during training and its reliability when tested with unseen data. On the other hand, Figure 7 presents the loss graph, showing how the loss value progressively decreases during training and validation. This information is crucial for understanding whether the model is experiencing underfitting or overfitting, as well as evaluating how well the model minimizes prediction errors. Next, Figure 8 displays the confusion matrix, which offers a visual representation of the model's prediction distribution across the test data for each class. The confusion matrix helps analyze errors by showing the number of correct and incorrect predictions for each class, making it possible to identify the classes that are most challenging for the model to predict. Furthermore, Figure 9 presents the AUC-ROC curve, which demonstrates the model's ability to distinguish between positive and negative classes. This curve visualizes the relationship between sensitivity and specificity, providing a strong indicator of how well the model handles class imbalance.

Based on the overall evaluation results, the DenseNet201 model with the application of CLAHE achieved the best performance with a batch size of 16, reaching the highest validation accuracy of 94.84%. This indicates that preprocessing with CLAHE has a significant positive impact in improving the model's ability to understand patterns in the data. For more detailed information, the evaluation results related to precision, recall, and F1-score can be found in Table 3.

P-ISSN: 2723-3863
E-ISSN: 2723-3871
Vol. 6, No. 2, April 2025, Page. 981-994
https://jutif.if.unsoed.ac.id
DOI: https://doi.org/10.52436/1.jutif.2025.6.2.4315

Table 3. Model performance Based on Precision, Recall, and F1-Score

Class	Precision	Recall	F1-Score
Normal	96.13%	0.9351	94.80%
Tuberculosis	93.59%	0.9618	94.87%

These visualizations not only provide information about the model's accuracy and stability during training, but also show how well the model predicts data and distinguishes between classes overall. These visualizations can be seen in more detail in Figures 6, 7, 8, and 9.

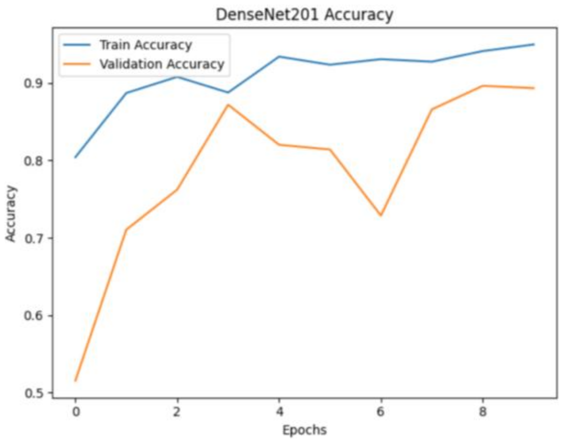

Figure 6. Accuracy Graph

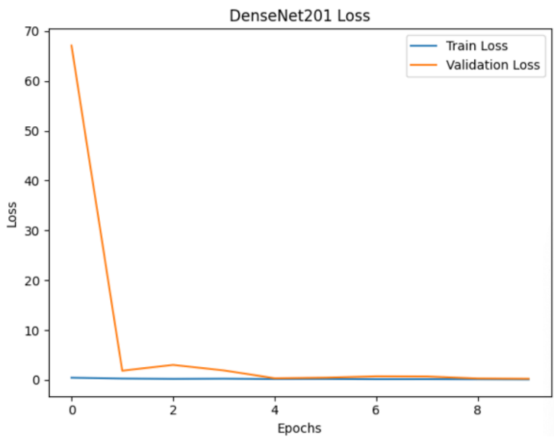

Figure 7. Loss Graph

The graphs in Figures 6 and 7 illustrate the performance of the DenseNet201 model during the training and validation processes. In Figure 6 (accuracy graph), the blue line represents the training accuracy, which steadily increases, indicating that the model is learning well from the training data. The orange line shows the validation accuracy, which initially improves well but experiences fluctuations at epoch 6, before showing improvement again in the following epochs.

Meanwhile, in Figure 7 (loss graph), the blue line represents the training loss, which consistently decreases as the epochs increase, indicating a reduction in prediction errors on the training data. The orange line represents the validation loss, which experiences a slight spike at epoch 2 but then decreases significantly, reflecting the model's improved generalization ability. Overall, the DenseNet201 model demonstrates excellent performance with high accuracy and low loss, highlighting its ability to learn data patterns and make effective predictions.

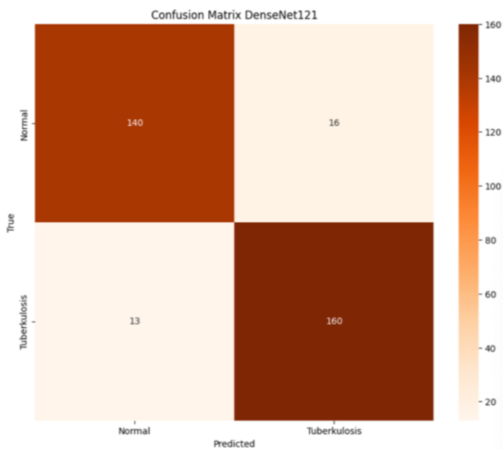

Figure 8. Confusion Matrix

P-ISSN: 2723-3863 https://jutif.if.unsoed.ac.id
E-ISSN: 2723-3871 DOI: https://doi.org/10.52436/1.jutif.2025.6.2.4315

The model evaluation using the confusion matrix aims to assess the performance of the deep learning or machine learning model in determining whether the predictions made are correct or incorrect based on the entire dataset used [33]. The confusion matrix in Figure 8 shows the performance of the DenseNet201 model in classifying two categories: Normal and Tuberculosis. The model successfully identified 140 samples in the Normal category and 160 samples in the Tuberculosis category. However, there were 16 samples from the Normal category that were misclassified as Tuberculosis (False Positives) and 13 samples from the Tuberculosis category that were misclassified as Normal (False Negatives). These results indicate that the model achieved a high accuracy level, demonstrating strong performance in distinguishing between the two categories.

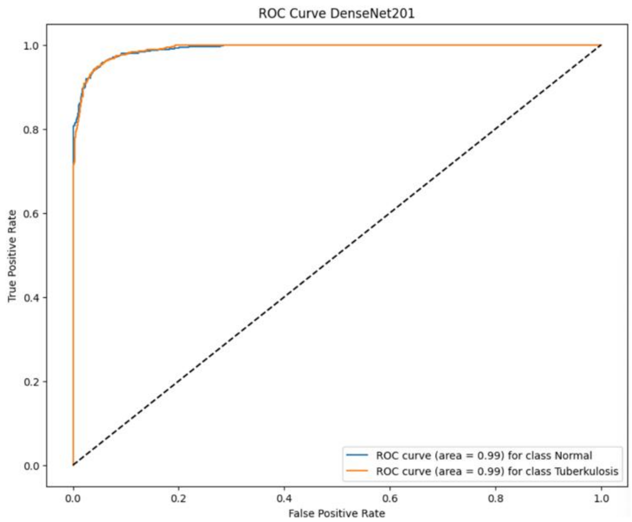

Figure 9. DenseNet201 Model AUC-ROC Curve

The AUC-ROC curve is an evaluation tool used to assess the performance of a model in classification tasks across various threshold settings. ROC (Receiver Operating Characteristic) is a curve that represents prediction probabilities, while AUC (Area Under the Curve) measures the model's ability to distinguish between classes. The AUC value provides an overview of how well the model can differentiate between categories. A higher AUC value indicates that the model is more effective in identifying class 0 as 0 and class 1 as 1, or, analogously, the better the model is at distinguishing one category from another [34].

Figure 8 illustrates the ROC curve for the DenseNet201 model in classifying two categories: Normal and Tuberculosis. Both curves show excellent performance, with an AUC value of 0.99 for each category. This value reflects the model's very high classification capability, with optimal sensitivity and specificity across various thresholds. These results confirm that the DenseNet201 model performs exceptionally well in distinguishing between the Normal and Tuberculosis categories.

4. DISCUSSION

Research on tuberculosis diagnosis using CNN has also shown promising results. A study by [11] using CNN with several architectures for tuberculosis diagnosis achieved an accuracy of 90%. A study conducted by [14] explored the application of CNN with five variants of EfficientNet architectures implemented on two datasets and achieved the highest accuracy with the EfficientNet-B4 model, 92.33% and 94.35%, respectively.

Research on the DenseNet201 model has also shown promising results. A study by [35] developed an algorithm using ensemble techniques to improve the accuracy and reliability of the DenseNet201 model in diagnosing lung diseases. A study by [36] used the DenseNet201 model to detect COVID-19

Vol. 6, No. 2, April 2025, Page. 981-994
P-ISSN: 2723-3863
https://jutif.if.unsoed.ac.id
E-ISSN: 2723-3871
DOI: https://doi.org/10.52436/1.jutif.2025.6.2.4315

and pneumonia from chest X-ray images, achieving an accuracy of 99.1%. Another study by [37] used a modified DenseNet201 model with additional convolutional layers for detecting skin cancer, achieving an accuracy of 95.50%. In [30], a study on disease classification in rice leaves using DenseNet201 achieved an accuracy of 88.33%.

Research on contrast enhancement with CLAHE has also shown promising results. A study by [15] improved medical image segmentation accuracy using CLAHE, showing accuracy improvement on chest X-ray and CT-Scan lung datasets. A study by [38] used CLAHE to enhance fundus retinal image quality, resulting in significant accuracy improvements in CNN models such as VGG16, InceptionV3, and EfficientNet. A study by [21] used CLAHE for brain cancer diagnosis, achieving an accuracy of 90.37%.

These findings are consistent with those conducted by [21], [15] and [38], which show that contrast enhancement methods improve the effectiveness of model classification. In this study, testing results indicated a 2.62% accuracy improvement using the CLAHE method. Previous research, as reported in [15], found that CLAHE improved accuracy by 2.73% on chest X-ray datasets and 0.66% on CT-Scan lung datasets. Another study, reported in [39], also showed that CLAHE could increase accuracy by 0.1%.

The results of this study suggest that CNN holds great potential in disease diagnosis based on medical images, but its application in real-world medical systems requires several considerations. Models must be tested with real-world data reflecting various patient conditions and image quality to ensure reliability. Furthermore, although the model shows high performance on specific datasets, further testing on datasets from different hospitals and regions is necessary to assess generalizability. Implementation in electronic medical record (EMR) systems also requires supporting infrastructure and compliance with data security and privacy regulations. Additionally, factors such as image quality variation, image artifacts, and data distribution across hospitals can impact model performance. Therefore, models must be developed with these aspects in mind to be accurate not only in laboratory testing but also effective in clinical practice.

5. CONCLUSION

Based on the results of applying CLAHE and the DenseNet201 architecture, as well as the analysis conducted, this study demonstrates that the application of effective preprocessing techniques, such as CLAHE, can have a significant positive impact on model performance in image classification tasks. The dataset with CLAHE applied showed better results compared to the dataset without CLAHE, as indicated by the improved performance of the model on the dataset with CLAHE. Additionally, experiments showed that batch size affects various training metrics, such as training accuracy, training loss, validation accuracy, and validation loss. While larger batch sizes can speed up training, smaller batch sizes do not always result in worse performance and often provide the best accuracy, as seen with a batch size of 16, which resulted in the highest accuracy. The model with CLAHE applied at the 10th epoch and batch size 16 showed the best test results, with an accuracy of 94.84%, indicating that the right combination of preprocessing and optimal model configuration is crucial for achieving more accurate and stable results. However, there are some limitations, such as the limited dataset variety used and the focus on a single model architecture. Therefore, further development could include exploring more diverse datasets, testing other model architectures, and applying additional preprocessing techniques to optimize model performance. This study contributes significantly to the fields of Informatics and Computer Science, especially in the development of deep learning models for medical image classification, and opens up opportunities for further research that could enhance the accuracy and generalization ability of models in real-world applications.

P-ISSN: 2723-3863 https://jutif.if.unsoed.ac.id
E-ISSN: 2723-3871 DOI: https://doi.org/10.52436/1.jutif.2025.6.2.4315

REFERENCES

[1] S. N. Hankare And S. S. Shirguppikar, "Detection Of Tuberculosis And Lung Cancer Using Cnn," In *Handbook Of Smart Materials, Technologies, And Devices: Applications Of Industry 4.0: Volume 1-3*, Vol. 2, 2022. Doi: 10.1007/978-3-030-84205-5_134.

[2] W. Zhou *Et Al.*, "Deep Learning-Based Pulmonary Tuberculosis Automated Detection On Chest Radiography: Large-Scale Independent Testing," *Quant Imaging Med Surg*, Vol. 12, No. 4, Pp. 2344–2355, Apr. 2022, Doi: 10.21037/Qims-21-676.

[3] World Health Organization, Regional Strategic Plan Towards Ending Tb In The Who South-East Asia Region : 2021-2021. 2021.

[4] M. Halim, A. Sabrina, And M. Aris Sekolah Tinggi Ilmu Kesehatan Ikifa, "Kepatuhan Pasien Rawat Jalan Poli Paru Dalam Penggunaan Obat Anti Tuberkulosis (Oat) Di Rumah Sakit Kartika Husada Jatiasih Bekasi," *Jurnal Farmasi Ikifa*, Vol. 2, No. 1, 2023.

[5] C. Zuo *Et Al.*, "Deep Learning In Optical Metrology: A Review," 2022. Doi: 10.1038/S41377-022-00714-X.

[6] L. Mohammadpour, T. C. Ling, C. S. Liew, And A. Aryanfar, "A Survey Of Cnn-Based Network Intrusion Detection," 2022. Doi: 10.3390/App12168162.

[7] D. Alsaeed And S. F. Omar, "Brain Mri Analysis For Alzheimer's Disease Diagnosis Using Cnn-Based Feature Extraction And Machine Learning," *Sensors*, Vol. 22, No. 8, 2022, Doi: 10.3390/S22082911.

[8] B. Tugrul, E. Elfatimi, And R. Eryigit, "Convolutional Neural Networks In Detection Of Plant Leaf Diseases: A Review," 2022. Doi: 10.3390/Agriculture12081192.

[9] T. T. Alemayoh, M. Shintani, J. H. Lee, And S. Okamoto, "Deep-Learning-Based Character Recognition From Handwriting Motion Data Captured Using Imu And Force Sensors," *Sensors*, Vol. 22, No. 20, 2022, Doi: 10.3390/S22207840.

[10] J. Qiang, D. Wu, H. Du, H. Zhu, S. Chen, And H. Pan, "Review On Facial-Recognition-Based Applications In Disease Diagnosis," 2022. Doi: 10.3390/Bioengineering9070273.

[11] E. Showkatian, M. Salehi, H. Ghaffari, R. Reiazi, And N. Sadighi, "Deep Learning-Based Automatic Detection Of Tuberculosis Disease In Chest X-Ray Images," *Pol J Radiol*, Vol. 87, No. 1, 2022, Doi: 10.5114/Pjr.2022.113435.

[12] T. Rahman *Et Al.*, "Reliable Tuberculosis Detection Using Chest X-Ray With Deep Learning, Segmentation And Visualization," *Ieee Access*, Vol. 8, Pp. 191586–191601, 2020, Doi: 10.1109/Access.2020.3031384.

[13] M. Nijiati *Et Al.*, "Artificial Intelligence Assisting The Early Detection Of Active Pulmonary Tuberculosis From Chest X-Rays: A Population-Based Study," *Front Mol Biosci*, Vol. 9, Apr. 2022, Doi: 10.3389/Fmolb.2022.874475.

[14] M. Oloko-Oba And S. Viriri, "Ensemble Of Efficientnets For The Diagnosis Of Tuberculosis," *Comput Intell Neurosci*, Vol. 2021, 2021, Doi: 10.1155/2021/9790894.

[15] S. Saifullah And R. Drezewski, "Modified Histogram Equalization For Improved Cnn Medical Image Segmentation," In *Procedia Computer Science*, 2023. Doi: 10.1016/J.Procs.2023.10.295.

[16] M. Zheng And W. Luo, "Underwater Image Enhancement Using Improved Cnn Based Defogging," *Electronics (Switzerland)*, Vol. 11, No. 1, 2022, Doi: 10.3390/Electronics11010150.

[17] S. Roy, M. Tyagi, V. Bansal, And V. Jain, "Svd-Clahe Boosting And Balanced Loss Function For Covid-19 Detection From An Imbalanced Chest X-Ray Dataset," *Comput Biol Med*, Vol. 150, 2022, Doi: 10.1016/J.Compbiomed.2022.106092.

[18] S. A. Widiarto, W. A. Saputra, And A. R. Dewi, "Klasifikasi Citra X-Ray Toraks Dengan Menggunakan Contrast Limited Adaptive Histogram Equalization Dan Convolutional Neural Network (Studi Kasus: Pneumonia)," *Jipi (Jurnal Ilmiah Penelitian Dan Pembelajaran Informatika)*, Vol. 6, No. 2, 2021, Doi: 10.29100/Jipi.V6i2.2102.

[19] R. K. Hapsari, M. I. Utoyo, R. Rulaningtyas, And H. Suprajitno, "Comparison Of Histogram Based Image Enhancement Methods On Iris Images," In *Journal Of Physics: Conference Series*, 2020. Doi: 10.1088/1742-6596/1569/2/022002.

Vol. 6, No. 2, April 2025, Page. 981-994
https://jutif.if.unsoed.ac.id
DOI: https://doi.org/10.52436/1.jutif.2025.6.2.4315

[20] Erwin And D. R. Ningsih, "Improving Retinal Image Quality Using The Contrast Stretching, Histogram Equalization, And Clahe Methods With Median Filters," *International Journal Of Image, Graphics And Signal Processing*, Vol. 12, No. 2, 2020, Doi: 10.5815/Ijigsp.2020.02.04.

[21] S. Aulia And D. Rahmat, "Brain Tumor Identification Based On Vgg-16 Architecture And Clahe Method," *International Journal On Informatics Visualization*, Vol. 6, No. 1, 2022, Doi: 10.30630/Joiv.6.1.864.

[22] Kamal And H. Ez-Zahraouy, "A Comparison Between The Vgg16 , Vgg19 And Resnet50 Architecture Frameworks For Classi Cation Of Normal And Clahe Processed Medical Images," 2023.

[23] R. M. Diar, R. Y. N. Fu'adah, And K. Usman, "Klasifikasi Penyakit Paru-Paru Berbasis Pengolahan Citra X Ray Menggunakan Convolutional Neural Network (Classification Of The Lung Diseases Based On X Ray Image Processing Using Convolutional Neural Network)," *E-Proceeding Of Engineering*, Vol. 9, No. 2, 2022.

[24] A. Alhudhaif, K. Polat, And O. Karaman, "Determination Of Covid-19 Pneumonia Based On Generalized Convolutional Neural Network Model From Chest X-Ray Images," *Expert Syst Appl*, Vol. 180, Oct. 2021, Doi: 10.1016/J.Eswa.2021.115141.

[25] F. Hussein *Et Al.*, "Hybrid Clahe-Cnn Deep Neural Networks For Classifying Lung Diseases From X-Ray Acquisitions," *Electronics (Switzerland)*, Vol. 11, No. 19, 2022, Doi: 10.3390/Electronics11193075.

[26] S. S. M. Sheet, T. S. Tan, M. A. As'ari, W. H. W. Hitam, And J. S. Y. Sia, "Retinal Disease Identification Using Upgraded Clahe Filter And Transfer Convolution Neural Network," *Ict Express*, Vol. 8, No. 1, 2022, Doi: 10.1016/J.Icte.2021.05.002.

[27] R. Fan, X. Li, S. Lee, T. Li, And H. L. Zhang, "Smart Image Enhancement Using Clahe Based On An F-Shift Transformation During Decompression," *Electronics (Switzerland)*, Vol. 9, No. 9, 2020, Doi: 10.3390/Electronics9091374.

[28] M. B. Kurniwan And E. Utami, "Comparative Analysis Of Contrast Enhancement Methods For Classification Of Pekalongan Batik Motifs Using Convolutional Neural Network," *Jurnal Teknik Informatika (Jutif)*, Vol. 5, No. 6, Pp. 1779–1787, 2024, Doi: 10.52436/1.Jutif.2024.5.6.2621.

[29] T. Mao And D. X. Zhou, "Rates Of Approximation By Relu Shallow Neural Networks," *J Complex*, Vol. 79, 2023, Doi: 10.1016/J.Jco.2023.101784.

[30] A. D. Saputra, D. Hindarto, And H. Santoso, "Disease Classification On Rice Leaves Using Densenet121, Densenet169, Densenet201," *Sinkron*, Vol. 8, No. 1, 2023, Doi: 10.33395/Sinkron.V8i1.11906.

[31] S. Majumdar, P. Pramanik, And R. Sarkar, "Gamma Function Based Ensemble Of Cnn Models For Breast Cancer Detection In Histopathology Images," *Expert Syst Appl*, Vol. 213, 2023, Doi: 10.1016/J.Eswa.2022.119022.

[32] S. Coulibaly, B. Kamsu-Foguem, D. Kamissoko, And D. Traore, "Deep Convolution Neural Network Sharing For The Multi-Label Images Classification," *Machine Learning With Applications*, Vol. 10, 2022, Doi: 10.1016/J.Mlwa.2022.100422.

[33] P. Ghose, M. A. Uddin, U. K. Acharjee, And S. Sharmin, "Deep Viewing For The Identification Of Covid-19 Infection Status From Chest X-Ray Image Using Cnn Based Architecture," *Intelligent Systems With Applications*, Vol. 16, 2022, Doi: 10.1016/J.Iswa.2022.200130.

[34] Ismai, "Machine Learning: Teori, Studi Kasus, Dan Implementasi Menggunakan Phyton," 2021.

[35] A. Sayeed *Et Al.*, "An Effective Screening Of Covid-19 Pneumonia By Employing Chest X-Ray Segmentation And Attention-Based Ensembled Classification," *Iet Image Process*, Vol. 18, No. 9, Pp. 2400–2416, Jul. 2024, Doi: 10.1049/Ipr2.13106.

[36] H. A. Sanghvi, R. H. Patel, A. Agarwal, S. Gupta, V. Sawhney, And A. S. Pandya, "A Deep Learning Approach For Classification Of Covid And Pneumonia Using Densenet-201," *Int J Imaging Syst Technol*, Vol. 33, No. 1, 2023, Doi: 10.1002/Ima.22812.

[37] M. Zia Ur Rehman, F. Ahmed, S. A. Alsuhibany, S. S. Jamal, M. Zulfiqar Ali, And J. Ahmad, "Classification Of Skin Cancer Lesions Using Explainable Deep Learning," *Sensors*, Vol. 22, No. 18, 2022, Doi: 10.3390/S22186915.

[38] A. Wanto, Y. Yuhandri, And O. Okfalisa, "Optimization Accuracy Of Cnn Model By Utilizing Clahe Parameters In Image Classification Problems," In *Proceedings - 2023 International*

Vol. 6, No. 2, April 2025, Page. 981-994
https://jutif.if.unsoed.ac.id
DOI: https://doi.org/10.52436/1.jutif.2025.6.2.4315

Conference On Networking, Electrical Engineering, Computer Science, And Technology, Iconnect 2023, 2023. Doi: 10.1109/Iconnect56593.2023.10327100.
[39] S. Hadiyoso, S. Aulia, And I. D. Irawati, "Diagnosis Of Lung And Colon Cancer Based On Clinical Pathology Images Using Convolutional Neural Network And Clahe Framework," *International Journal Of Applied Science And Engineering*, Vol. 20, No. 1, 2023, Doi: 10.6703/Ijase.202303_20(1).006.